Thin film preparation of silicon nanocrystals embedded in silicon oxide by sol-gel method

Thipwan Fangsuwannarak[1] and **Kanika Khunchana**[2], Non-members

ABSTRACT

In this paper, nano silicon powders were prepared by the grinding technique and subsequently mixed in sol-gel of Tetraethylorthosilicate and ethanol solution. The silicon dioxide films synthesized from the sol-gel solution were preliminary studied in the term of the optical property as a refractive index (n) by varying the aging time and annealing temperatures. By using a Fourier transform infrared spectroscopy technique, the obtained x-composition values of the SiO_x films were extended from 1.67 to 1.98 with a decreasing time of the aged sol-gels. In addition, the lower x-composition value can be controlled by increasing the annealing temperatures from 60°C to 500°C. The prepared films from the precursor of nano-silicon powder suspension were characterized by photoemission spectroscopy and Raman spectroscopy in order to obtain more understanding of the chemical composition and silicon nano-crystallite quality, respectively. Presenting the spectra broadening and the frequency downshifting from 521 cm^{-1} was caused by the quantum size effect.

Keywords: Silicon, Nanocrystals, Thin Film, Sol-gel, Silicon Oxide

1. INTRODUCTION

Photonic devices such as light emitting diodes (LEDs) and lasers seem to be impossible to exploit a silicon (Si) material as an optically active layer due to its indirect band gap. Nowadays, there are many breakthroughs in the utilization of more photonic functions of nano-crystalline Si (nc-Si) material [1]. The quantum confinement effect of charge excitons in the silicon nanostructure leads to a quasi-direct transition [2]. In addition, by forming the Si low-dimensional system, the main reason is its compatibility with the fabrication technology of integrated circuits.

The quantum confinement effect in Si nanostructures constitutes another approach to engineering a quasi-direct transition and the visible light emission at room temperature. In particular, the nc-Si band gap can be extended due to shifting down of the valence states and shifting up of the conduction states in energy when the small nanometric size approaches the size of its Bohr exciton radius. The band gap shift due to the quantum confinement will be $\Delta Eg \propto 1/(m^* a^2)$ in a simple effective mass approximation, where m^* is an effective isotropic mass in the confinement direction, and a is a nanoparticle size. For promising nano-optoelectronic devices, the recombination mechanisms of nc-Si material at room temperature which are caused by the size confinement play a vital part [3]: Shockley-Read-Hall recombination is suppressed because carriers become localized and are not able to diffuse to defects. Auger recombination is not present until two excitons are generated within the same nanocrystals. Furthermore, radiative recombination becomes more efficient since the electron-hole wavefunctions overlap overwhelmingly in space causing faster recombination. These recombination behaviors have led to been widely investigated in the structural, electronic, and optical properties of nanocrystal materials. Especially, the systems composed of nc-Si embedded into its dielectric materials such as its oxides, nitrides, and carbides. They present a promising alternative to tunable band gap from 1.2- 2.0 eV [4].

A variety of different fabrication techniques have been used to produce such Si quantum dot material which is compatible with the standard Si technology. The techniques include ion implantation [5-6], plasma enhanced chemical vapor deposition (PECVD) [7], and RF magnetron sputtering and followed by high temperature annealing [8]. The problem here is the difficulty in achieving concentrations high enough to obtain efficient optical properties. Many techniques have been expensive and time consuming because of the production under high vacuum and/or annealing processes. A sol-gel method is quite inexpensive and easy to fabricate such Si nanocrystals embedded into its dielectric matrix. The sol-gel method by centrifugal processing has been suggested as a technique to be achieved in this objective [9]. The sol-gel was used as a viscous medium through Si crystallites settle. Nonetheless, the centrifugal processing might produce a bulk material which has such a functional limitation for thin film optoelectronic devices.

In this paper, by sol-gel spin coating technique, we prepared nc-Si thin films in the formation of

Manuscript received on August 15, 2012 ; revised on February 20, 2013.

Final manuscript received May 9, 2013.

[1,2] The authors are with School of Electrical Engineering, Institute of Engineering, 1Suranaree University of Technology Muang District, Nakhon Ratchasima, Thailand 30000, E-mail: thipwan@g.sut.ac.th

[1] Corresponding author. Tel +66 44224582 e-mail : thipwan@g.sut.ac.th (T. Fangsuwannarak)

nanocomposite materials. The prepared silicon nanostructure consists of the nano-Si powders, which were dispersed in a continuous silicon dioxide phase. *P*-type (100) Si wafer as nano-Si powders precursor was appropriately grinded for our work. The prepared SiO2 buffer layer by synthesizing the sol-gel is a crucial stack of the layers for our work. Furthermore, the investigation step of boron doped in the nc-Si dots/SiO_2 film is a very important towards a realization of a nano-scaled $p-n$ junction device. For a compositional analysis, the chemical bonding environment of boron was investigated by the photoemission spectroscopy (PES). The crystal structure of nanometer Si dots embedded into the silicon oxide was studied by the measurement of Raman spectra.

2. EXPERIMENTAL PROCEDUE

2.1 Synthesis of nano-crystalline Si thin films by sol-gel technique

Under long time of the grinding process, the nano-Si powders were produced from a mono-crystalline *p*-type Si wafer with the boron impurity (1-20 Ω·cm, ¡100¿) in a mixture of ethanol absolute. The biggest Si particles were properly eliminated by filtering through a sieve with pore radius of 45 μm.

Tetraethylorthosilicate, $Si(OC_2H_5)_4$ (TEOS, 98% Fluka) and ethanol absolute, (C_2H_5OH, (99% BDH) (EtOH)) were used as a silicon oxide precursor. In fabrication of Si oxide buffer layer, the dielectric sol-gel was first prepared as follows: 1 mole of TEOS and 2 moles of EtOH were mixed and then stirred for 15 min at the room temperature. Cetyl Trimethyl Ammonium Bromide, $C_{19}H_{42}BrN$ (CTAB, 99% Sigma Aldrich) was used as surfactant. In addition, 0.0013M CTAB and 0.1M HCl catalysts in water were subsequently added dropwise to the solution until the water to TEOS molar ratio of 2. The condensation of TEOS at about pH 2 was controlled by adding HCl catalyst. The proper solutions were then stirred at room temperature for 60 minutes.

In order to obtain the suspension uniformity, sol-suspension was prepared from mixture of nano-scaled Si powders (0.05 g) with TEOS solution (5ml) under an ultrasonic for 30 min. The preparing process of sol-suspension is shown in Fig. 1.

In our work, different substrates (fused quartz and Si wafer) were used for an aim of different measurements. After cleaning the Si wafers and quartz substrates by a RCA process, particular Si wafers were dipped in dilute 5% hydrofluoric solution and rinsed in deionized water in order to remove the native oxide on the surface. After aging of the gel for 1 day, the prepared TEOS gel as a Si oxide precursor was spun at 2000 rpm for 20 s. on the Si substrate. The obtained Si oxide is an important buffer layer in order to have a good coherence between its surface and the sol-suspension for the next process step. To prevent the crack of the gel structure, the first Si oxide film as a buffer film was suitably dried for 2 hours in an oven. Subsequently, sol-suspension deposition by spin-coating on a dried oxide buffer layer was released. Under properly sequence process, B-doped Si nanocrystallites embedded in a continuous oxide dielectric phase were expected to obtain in this work.

2.2 Characterizations of the thin films

Optical and structural characterizations of the SiOx layer deposited on a polished Si substrate were determined under various annealing temperatures by using an ellipsometer (L117, Gaertner Corp.) with a laser wavelength of 638 nm for refractive index and film thickness measurements. The stoichiometry of as-deposited SiO_x, with varying annealing temperature in the range of 60°C - 500°C , was estimated from shifts of the asymmetric Si-O-Si stretching peak with adjacent O-atoms in the IR absorption spectra. The change in chemical bonding state of Si oxide film was also analyzed by using Fourier transform infrared spectroscopy, FT-IR (Nicolet, 6700 ATR mode) with a wavenumber resolution of 2 cm-1. Photoemission spectroscopy with synchrotron light source was performed on the surface after Ar^+ ions sputter etching, with the fixed photon energy at 160eV (Si) and 270eV (B). The annealed films on quartz substrate, which have a composite of nc-Si dots embedded in SiO_x phase were identified the chemical compositions by the PES measurement. The spectra corresponding to the Si(2p) peak were analyzed to confirm the existence of B-Si bonding. The structural properties in nano-scale of the film on quartz were identified by Raman spectroscopy, which was obtained by using the 638.2 nm line of an Ar^+ laser. The laser power incident on the samples was reduced to minimum in order to avoid artifacts. The cross-sectional images of the film were further verified by Scanning electron microscopy (SEM, 1450VP, LEO).

3. RESULTS AND DISCUSSION

Refractive index of the prepared dielectric film is an important parameter to provide its optical information for a further photonic design. These results in Fig. 2 show the influence of annealing temperature on the thickness and refractive index values of the film. By increasing the temperature, the average value of the refractive index exhibits a slightly increase from 1.46 - 1.50. It could be contributed to the start of pore removal and densification which is similar to Fardad's work [10]. Nonetheless, the film thickness gradually shrinks from 150 nm to 90 nm. It is mainly due to the shrinkage of the gels during drying is forced by capillary pressure of the small pore liquid [11]. By annealing temperature, the surface tension between liquid and vapor cannot be avoided. Therefore, the less shrinkage of as-prepared film and also the film annealed at 60°C can lead to the less crack or crack free.

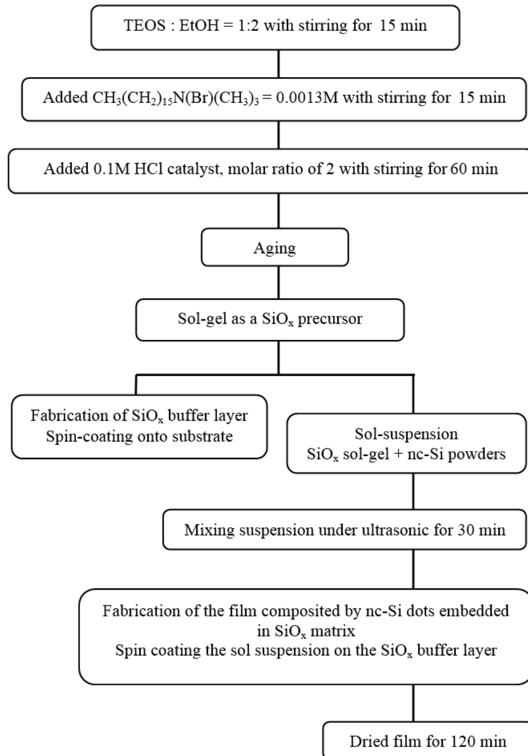

Fig.1: *Sol-gel processing schematic for preparing particulate Si suspension.*

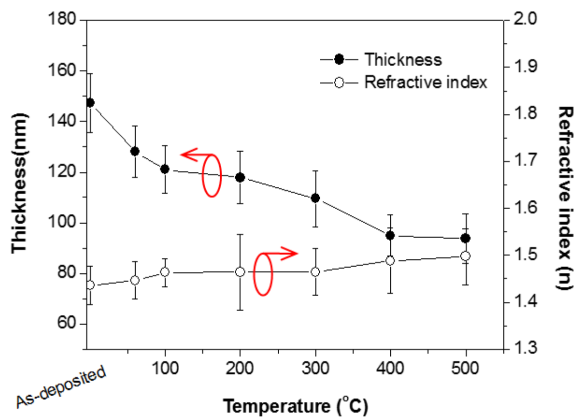

Fig.2: *Change of the thickness and the refractive index vs. annealing temperature.*

In Fig. 3, at low drying temperature (60 °C), the influence of the aging time of the gel on average thickness and refractive index of SiO_x film with the crack free gives a same tendency. With the longer aging time, the thickness increases as a consequence of a more gel viscosity. For 4-day gelation time, thickness and refractive index reversible drop possibly due to that EtOH as a solvent evaporates, causing shrinkage of the gel network. This behavior in our result is consistent with Dai et al. study [12]. The reflective index of the prepared film by the sol-gel technique presents in the range of 1.45-1.50.

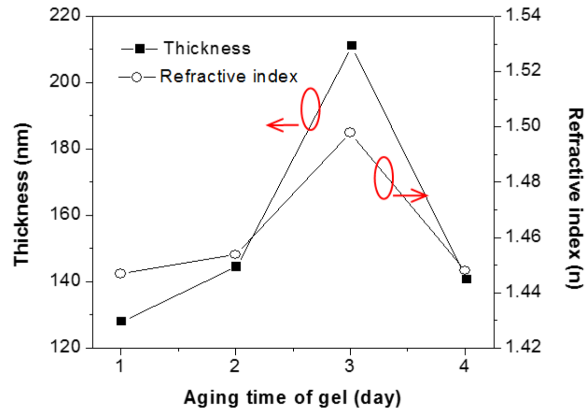

Fig.3: *Change of average thickness and refractive index of the SiO_x film with aging time of sol-gel precursor.*

The SiO_x films on polished Si wafer which annealed at 60 °C for different aging time of silica precursor were prepared for FTIR measurement. It was found that the system of low temperature annealing at 60°C has a similar tendency as shown in Fig.4. The main features of IR absorption of SiO_x are observed at Si-O rocking mode (460 cm^{-1}), the Si-O bending mode (800 cm^{-1}), the Si-O-Si stretch mode with adjacent O-atoms in phase (1000-1100 cm^{-1}) and with adjacent O-atom out of phase (1150-1200 cm^{-1}) [13]. The weak frequency band near 800 cm^{-1} can be indicated the ethanol skeletal vibration.

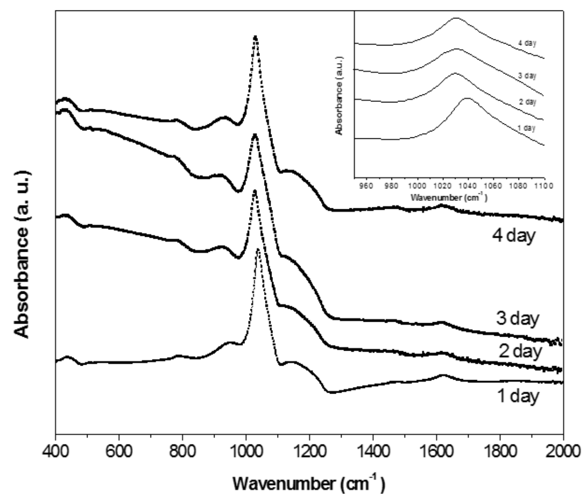

Fig.4: *FTIR spectra of the SiO_x film at the different stage of aging time of TEOS solution.*

Stoichiometry x of the SiO_x films was experimentally derived by elastic recoil detection (ERD) measurement of J. U. Schmidt [14] as presented in the relationship of the equation (1). From the plot in Fig. 5, it was found that the x-composition of the prepared SiO_x $(1 < x < 2)$ has a reverse tendency with refractive index and thickness of the SiO_x film.

$$v = 978.72 + 30.63x \quad (1)$$

where v is a position of peak frequency (cm^{-1}) and x is stoichiometry of SiO_x film.

Additionally, to receive information on the SiO_x under 1 day aging, the silica gel was prepared and spun on a polished Si wafer for the IR absorption measurement and subsequently annealed at different temperatures. FTIR absorption spectra of as-deposited and annealed films are reported in Fig. 6. It is notable that the strongest frequency peak at around 1028-1041cm^{-1}, which is related to its Si-O-Si stretch mode, shifts toward lower in wavenumbers when the as-deposited SiO_x films were heated at the higher temperature. The appearance of the spitting band and shoulder band in the region of 1100-1200 cm^{-1} was explained from the several different reasons. According to C. T. Kirk [15], these two bands are related to the out-of-phase motion of adjacent oxygen atoms with respect to the central Si atom due to the mechanical coupling between these longitudinal optic (LO) and transverse optic (TO) vibrational modes.

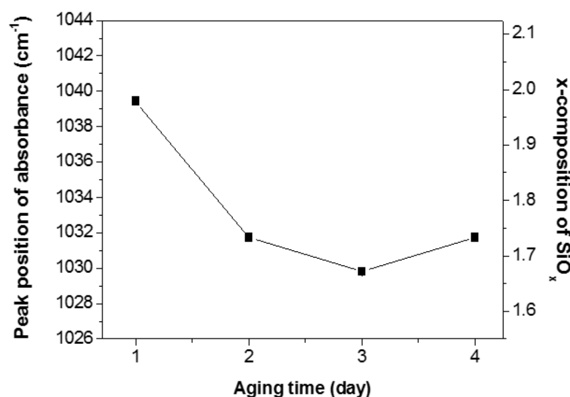

Fig.5: *Plot of frequency peak position and x-composition of the SiO_x film with different aging time of sol-gel precursor.*

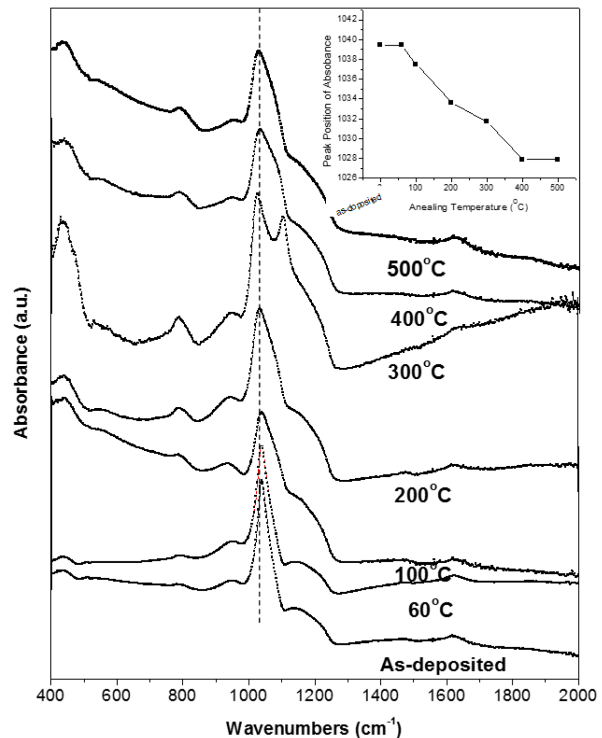

Fig.6: *FTIR spectra of thin film SiO_x at different stage of heat treatment.*

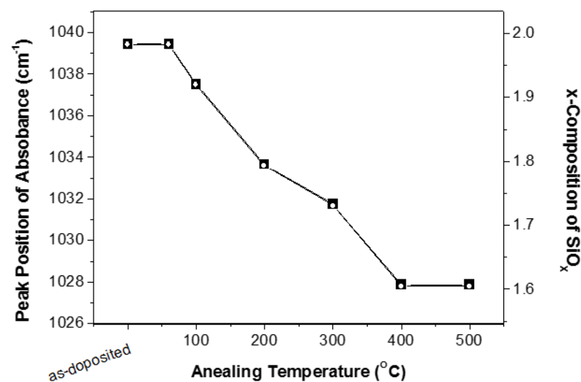

Fig.7: *Plot of frequency peak position and x-composition of the SiO_x films with different annealing temperature.*

In Fig.7, the empirical data of x-stoichiometry in the SiO_x for the different annealing temperature were also determined. The x-stoichiometry data as a function of heat treatment is expected to be in the range of ∼1.60 - ∼2.0. For the system processed at low sintering, we apply the SiO_2 as a medium dielectric phase for nc-Si dots film.

Chemical composition of the film consisting of nc-Si powders embedded in SiO_2 phase was examined by the PES measurement. In Fig. 8, the PES spectra reveal the appearance of the B2s energy broad band around 185-190 eV and the SiO_2 peak around 103 eV for Si2p energy. The peak around 99 eV attributed to Si crystallites is hardly seen possibly due to very low photo-emission responsibility of nano-crystallites. The peak around 187 eV can be contributed to B-B and B-Si bonding which is presented in all annealed samples. For annealed sample at 400°C, the presence of B-O bonding at 193 eV occurred upon the high temperature annealing due to such boron out diffusion from B-B and/or B-Si environments at the high temperature annealing. Additionally, in Fig.9 the PES spectrum with the higher resolution step was examined the B-O bonding.

The thickness of as-deposited film layer was verified by cross-section SEM with dark field mode. It shows the clear monolayer structure deposited with a sol-gel coating, where thickness of the nc-Si dots and SiO_2 buffer layers are 1.5 μm and 0.15 μm, respec-

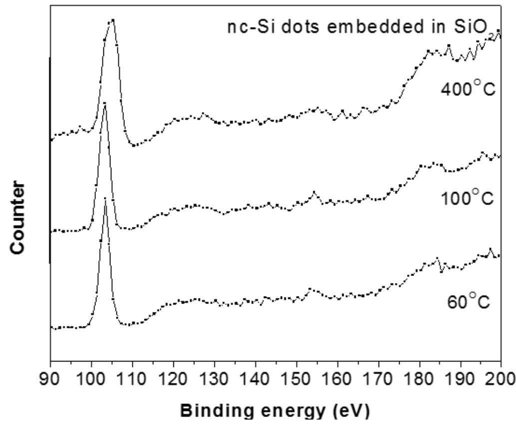

Fig.8: *PES Si2p and B2s spectra of the films consisting of nc-Si dots in SiO_2 phase with temperature annealing at 60° C, 100° C, and 400° C .*

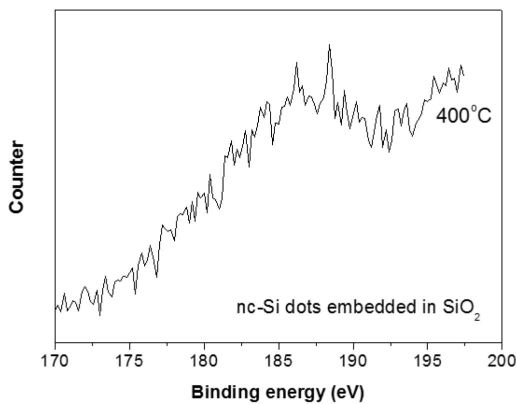

Fig.9: *PES B2s spectra with the resolution step of 0.20 eV of the films consisting of nc-Si dots in SiO_2 phase.*

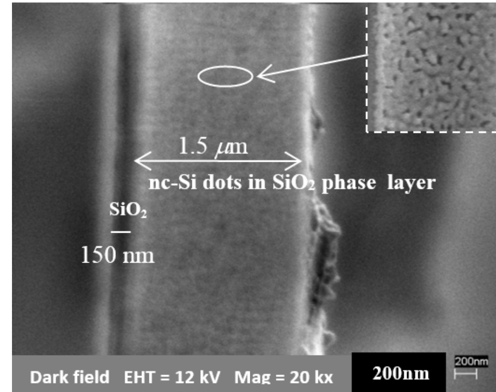

Fig.10: *SEM cross-section view of nano Si dots/SiO_2 film.*

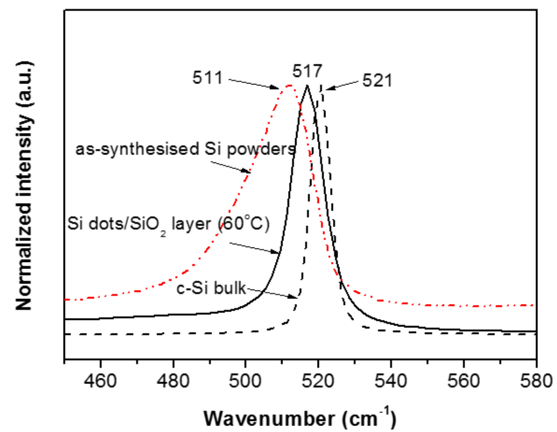

Fig.11: *Change of Raman frequency peak spectra of Si nanostructure materials with a Si bulk comparison.*

tively.

The quality of Si crystallinity and also crystal in nano-scale was typical investigated by micro-Raman spectroscopy. This is due to that the first-order (1TO mode) Raman spectrum is very sensitive at the atomic scale to structural modification. The Raman spectra in Fig. 10 show the main 1TO peak at 511, 517, and 521 cm^{-1} of as-synthesized Si powders, Si dots film, and bulk silicon as a reference sample, respectively. It was found that the spectral of Si nanostructure material become asymmetric broadening and the frequency peak shifts downward from 521 cm^{-1}. G. H. Loechelt *et al.*[16] suggested that the frequency shift and spectrum broadening are caused by stress and strain in the film. Nonetheless, following the model of Richter *et al.*[17] size confinement of results in uncertainty in the phonon momentum, thus leading to a downshift and asymmetric broadening of the first-order Raman spectrum.

For size approximation, we used the analytic equation (2) of Zi *et al.* [18] as followings

$$\Delta\omega = -A\left(\frac{a}{L}\right)^{\gamma}, \quad (2)$$

where A = 47.41 cm^{-1} , $\gamma = 1.44$, a is the silicon lattice parameter ($a = 0.543$ nm), L is silicon dot diameter, and $\Delta\omega$ is the shift frequency.

Average size of the synthesized Si powder and the nc-Si dots in SiO_2 is of ~3 nm and ~1.6 nm, respectively.

4. CONCLUSION

In this work, the process was prepared by using the sol-gel technique in order to produce nc-Si dots film by spin-coating method. Several characterization techniques was applied to the study of nanomaterial structures consisting of nc-Si dots embedded in a SiO_2 phase. Furthermore, the results from refractive index and FTIR measurement suggested the optimal film preparation at 1 day aging gel of the oxide sol-gel. We also achieve to prepare the thin film of with crack-free consisting of nc-Si dots in a SiO_2 phase. The nc-Si powder was fabricated by grinding p-type Si wafer. PES analysis revealed possible boron incorporation

in nc-Si films. We expect to have the presence of B-Si bonding for further conductivity improvement. Thus, the appropriate annealing of nc-Si dots is under a low temperature owing to the weak of B-O bonding. Si dots film was observed by SEM. The obtained nc-Si films consisted of the nc-Si dots show the good quality of the Si crystal be implied by the Raman spectroscopy measurement.

5. ACKNOWLEDGEMENT

This work was supported by Suranaree University of Technology, Thailand under the 2010 grant. The authors greatly acknowledge the beam line 3.2a (PES), Siam photon Laboratory, synchrotron light research institute, Thailand for use of their resources.

References

[1] Z.H. Lu, D.J. Lockwood, and J.M. Baribeau, "Quantum confinement and light emission in SiO2/Si superlattices" *Nature*, 378, pp. 359, 1995.

[2] M. Peŕalvarez, J. Barreto, J. Carreras, A.Morales,D.N. Urrios, Y. Lebour, C.Domìnguez, and B Garrido, "Si-nanocrystal-based LEDs fabricated by ion implantation and plasma-enhanced chemical vapour deposition," *Nanotechnology* ,20, 405201, 2009.

[3] J. Linnros, "Silicon-based microphotonics from basics to applications," *IOS Press*, Amsterdam, pp. 47-85, 1999.

[4] G. F. Grom, D. J. Lockwood, J. P. McCaffrey, H. J. Labbe, P. M. Fauchet, B. White, Jr., J. Diener, D. Kovalev, F. Koch, and L. Tsybeskov, *Nature*, 407, pp. 358 2000.

[5] K.S. Min, K.V. Shcheglov, C.M. Yang, H.A. Atwater, M.L. Brongersma, and A. Polman, "Defect-related versus excitonic visible light emission from ion beam synthesized Si nanocrystals in SiO2," *Applied Physical Letters*, 69, pp. 2033-2035., 1996.

[6] M. Perålvarez, C. García, M. López, B. Garrido, J. Barreto, C. Dom?nguez, and J.A. Rodr?guez, "Field effect luminescence from Si nanocrystals obtained by plasma-enhanced chemical vapor deposition,"*Applied Physical Letters*, 89, 051112/1-051112/3., 2006.

[7] F. Iacona, C. Bongiorno, C. Spinella, S. Boninelli, and F. Priolo, "Formation and evolution of luminescent Si nano clusters produced by thermal annealing of SiO_x films," *Journal of Applied Physics*, 95, pp. 3723-3732, 2004.

[8] P.M. Fauchet, J. Ruan, H. Chen, L. Pavesi, L. Dal Negro, M. Cazzaneli, R.G. Elliman, N. Smith, M. Samoc, and B. Luther-Davies, "Optical gain in different silicon nanocrystal systems," *Optical Materials*, 27, pp.745-749, 2005.

[9] D.J. Duval, B.J. McCoy, S.H. Risbud, Z.A. Munir, "Size selected silicon particles in sol-gel glass by centrifugal processing," *Journal of Applied Physics*, 83, pp. 2301-2307, 1998.

[10] M. A. Fardad, "Catalysts and the structure of SiO_2 sol-gel films," *Journal of Materials Science*, 35, pp. 1835-1841, 2000.

[11] A. Soleimani Dorcheh, and M.H. Abbasi, "Silica aerogel; synthesis, properties and characterization", *Journal of materials processing technology*, 199, pp. 10-26, 2008.

[12] S. Dai, Y. H. Ju, H. J. Gao, J. S. Lin, S. J. Pennycook, and C. E. Barnes, *Chem. Commun.*, pp. 243, 2000.

[13] A. Lehmann, L. Schunmann, and K. Huebner, "Optical Phonons in Amorphous Silicon Oxides. I. Calculation of the Density of States and Interpretation of Lo_To Splittings of Amorphous SiO2," *Physica Status Solidi B117*, pp.689-698, 1983.

[14] J. U. Schmidt, and B. Schmidt, "Investigation of Si nanocluster formation in sputter-deposited silicon sub-oxides for nanocluster memory structures," *Materials Science and Engineering B101*, pp.28-33, 2003.

[15] C. T. Kirk, "Quantitative analysis of the effect of disorder-induced mode coupling on infrared absorption in silica," *Physic Review B*, 38, pp. 1255-1273, 1988.

[16] G. H. Loechelt, N. G. Cave, and J. Menendez, "Measuring the tensor nature of stress in silicon using polarized off-axis Raman spectroscopy," *Applied Physical Letters*, 66, pp. 3639, 1995

[17] H. Richter, Z. P. Wang, and L. Ley, "The one phonon Raman Spectrum in microcrystalline silicon", *Solid stat commun.*, 39, pp. 625, 1981.

[18] J. Zi, H. Bscher. C. Falter, W. Ludwig, K. Zhang and X. Xie, "Raman shifts in Si nanocrystals," *Applied Physical Letters*, 69, pp.200,1 996.

Thipwan Fangsuwannarak is currently an Assistant Professor of Photovoltaic Engineering in the School of Electrical Engineering at Suranaree University of Technology, Thailand. She received her PhD degree from the University of New South Wales in 2008. Her research interests include photovoltaic fabrication, solar cell grid connection, standalone systems and energy harvesting systems.

Kannika Khunchana received her B.E. and M. E. degrees in Electrical Engineering from Suranaree University of Technology in 2010 and 2013, respectively. Her current research interests are nanosilicon material for new generation solar cell and opto-electric applications.